AD-A043 284 NAVAL RESEARCH LAB WASHINGTON D C F/G 20/9
LOW FREQUENCY INSTABILITY OF LIQUID LINER IMPLOSIONS DRIVEN BY --ETC(U)
JUN 77 A L COOPER, P J TURCHI

UNCLASSIFIED NRL-MR-3522 NL

1 OF 1
AD
A043 284

END
DATE FILMED
9-77
DDC

AD A043284

NRL Memorandum Report 3522

12
NW

Low Frequency Instability of Liquid Liner Implosions Driven by Multiple Free Pistons

A. L. Cooper
P. J. Turchi

Plasma Physics Division

June 1977

DDC
RECEIVED
AUG 24 1977
C

AD No.
DDC FILE COPY

NAVAL RESEARCH LABORATORY
Washington, D.C.

Approved for public release; distribution unlimited.

SECURITY CLASSIFICATION OF THIS PAGE (When Data Entered)

REPORT DOCUMENTATION PAGE

READ INSTRUCTIONS BEFORE COMPLETING FORM

1 REPORT NUMBER: NRL Memorandum Report 3522	2 GOVT ACCESSION NO.
3 RECIPIENT'S CATALOG NUMBER: NRL-MR-3522	
4 TITLE (and Subtitle): LOW FREQUENCY INSTABILITY OF LIQUID LINER IMPLOSIONS DRIVEN BY MULTIPLE FREE PISTONS	5 TYPE OF REPORT & PERIOD COVERED: Interim report on a continuing NRL/ERDA problem
	6 PERFORMING ORG. REPORT NUMBER
7 AUTHOR(s): A.L. Cooper and P.J. Turchi	8 CONTRACT OR GRANT NUMBER(s): USERDA E(49-20)-1009 ED-03-02
9 PERFORMING ORGANIZATION NAME AND ADDRESS: Naval Research Laboratory Washington, D.C. 20375	10 PROGRAM ELEMENT, PROJECT, TASK AREA & WORK UNIT NUMBERS: NRL Problem H02-28D RR 011 09 41
11 CONTROLLING OFFICE NAME AND ADDRESS	12 REPORT DATE: June 1977
	13 NUMBER OF PAGES: 20
14 MONITORING AGENCY NAME & ADDRESS (if different from Controlling Office)	15 SECURITY CLASS. (of this report): UNCLASSIFIED
	15a DECLASSIFICATION/DOWNGRADING SCHEDULE

16 DISTRIBUTION STATEMENT (of this Report)

Approved for public release; distribution unlimited.

DDC RECEIVED AUG 24 1977 C

17 DISTRIBUTION STATEMENT (of the abstract entered in Block 20, if different from Report)

18 SUPPLEMENTARY NOTES

19 KEY WORDS (Continue on reverse side if necessary and identify by block number)

Liner implosion
Hydrodynamic instability
Rayleigh-Taylor instability
Captive liner
Finite element surface

20 ABSTRACT (Continue on reverse side if necessary and identify by block number)

The Rayleigh-Taylor instability is studied for an unstable interface composed of rigid finite elements. For wave lengths associated with the finite element scale size the classical Rayleigh-Taylor growth rates obtain. Wave lengths which are short compared with the element scale size are constrained by the rigid finite elements. The consequences of this behavior are discussed with respect to captive liner configurations for imploding liners.

DD FORM 1 JAN 73 1473 EDITION OF 1 NOV 65 IS OBSOLETE
S/N 0102-014-6601

SECURITY CLASSIFICATION OF THIS PAGE (When Data Entered)

251 950

CONTENTS

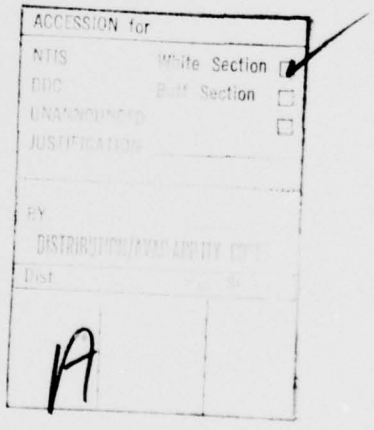

PRECEDING PAGE BLANK-NOT FILMED

Low Frequency Instability of Liquid Liner Implosions Driven by Multiple Free Pistons

I. Introduction

The use of imploding liquid cylinders or liners to compress plasma and/or magnetic flux to high energy densities has recently received considerable attention[1]. A basic problem inherent in such dynamic compression techniques is the growth of hydrodynamic perturbations at the free surfaces of the liner as these surfaces accelerate toward the higher mass density liquid in response to the pressures of the driving fluid (gas or magnetic field) and the payload plasma and/or field. Such growth is completely analogous to the phenomenon of Rayleigh-Taylor instability[2] in a gravitational field, and can result in both the disruption of the outer surface of the imploding liner during the initial implosion and the destruction of the high temperature plasma payload by inner surface material near peak compression. The latter effect can eliminate the liner implosion technique as a method of achieving fusion plasmas, while the former process severely limits the possibility of controlling and recovering the liner kinetic energy which is important in fusion reactor applications[3].

It has been shown theoretically[4,5] and demonstrated experimentally[6,7] that the Rayleigh-Taylor instability at the inner surface near peak

Note: Manuscript submitted May 31, 1977

compression can be eliminated by spinning the liner. During implosion, the azimuthal speed of the inner surface material increases, due to conservation of angular momentum, such that the centripetal acceleration ($-v^2/r$) overcomes the radial acceleration ($\ddot{r}$) to reverse the effective gravity at the interface ($\ddot{r} - v^2/r$) in favor of stability. Such rotation, however, does not remove the Rayleigh-Taylor instability at the outer surface when the liner is accelerated initially by a gas or magnetic pressure and similarly when it is decelerated after rebounding from peak payload compression.

To eliminate the Rayleigh-Taylor instability at the free outer surface, it was suggested[3] that the free outer surface itself be eliminated. The liner would be driven by free-pistons in continuous contact with the fluid, with the pistons providing a stiff interface between the high density liquid liner and a low density fluid drive, such as high pressure gas. The original concept was to use a flat disc or annulus displaced axially to drive the fluid. The first experimental arrangement, however, consisted of a plurality of free-pistons displaced radially inward to inject fluid into a central implosion chamber. This is shown schematically in Fig. 1. Experimental tests with such systems demonstrated that the outer surface instability was indeed subdued, with repetitive implosion-reexpansion cycles observed. It was pointed out[8], however, that the azimuthal array of free-pistons should be subject to Rayleigh-Taylor instability for wavelengths larger than the piston diameter. Experimentally, azimuthal asymmetries in the radial positions of the pistons are observed. While various processes can contribute to such asymmetries, it is useful to consider first the growth of positional variations due to hydrodynamic instability.

The analysis of the following section is similar in spirit to the classical Rayleigh-Taylor analysis but differs in that the interface between the heavy and light fluids consists of a stiff, thin plate displaced normal to its surface. A succession of such plates or pistons is displaced in a periodic manner to provide the initial condition of the boundary between the two fluids. In the classical Rayleigh-Taylor analysis, for each mode the interface is a sine or cosine wave. In the present work, the interface at any time appears as a train of square waves.

II. Model

From the above discussion, it is clear that the fundamental problem is that of the hydrodynamic or Rayleigh-Taylor instability of a surface comprised of finite elements. To isolate the main physics of this problem in its most simplified form, we neglect curvature and consider the situation depicted in Fig. 2. That is, we treat an infinite fluid slab of depth d in a constant vertical gravitational field g. The upper surface, $z = 0$, is taken to be a rigid wall. The lower surface $z = -d$ is taken to be composed of finite rigid elements of length ℓ in the x direction. This then represents a variation of the classical Rayleigh-Taylor instability problem where for a continuous free surface at $z = -d$ the surface perturbation growth rates, ω, satisfy[9]

$$\omega^2 = kg \tanh(kd) \qquad (1)$$

where k is the horizontal wave number of the disturbance $k = 2\pi/\lambda$ and λ is its wavelength. The shorter wavelength disturbances grow faster than the longer ones.

For the finite element surface configuration of Fig. 2, the situation is drastically changed. Now a constraint is imposed on the Fourier harmonics of the surface displacement to insure that the resultant surface is always consistent with the rigid finite elements of which it is composed. The dispersion relation for the free surface given by Eq. (1) is clearly not acceptable in this case.

We assume that the fluid slab is incompressible and inviscid and the region $z < -d$ is an extremely low density fluid so that hydrostatic pressure effects there are negligible. Consistent with the assumption of zero viscosity, we take the slab fluid motion to be irrotational.

III. Analysis

Since the flow field is irrotational, $\nabla \times \underline{q} = 0$, the velocity field is derivable from a potential

$$\underline{q} = \nabla\varphi(x,z,t) \tag{2}$$

Fluid incompressibility (ρ = constant) requires that

$$\nabla \cdot \underline{q} = 0 \tag{3}$$

or

$$\nabla^2 \varphi = 0 \tag{4}$$

Therefore, the velocity potential satisfies Laplace's equation within the slab. Equation (4) must be supplemented by the associated boundary conditions in order to solve for φ. At $z = 0$, rigid wall, the vertical component of velocity must vanish

$$\frac{\partial\varphi}{\partial z}\,(z = 0) = 0 \tag{5}$$

At the lower surface, $z = -d$, we must proceed with care. The kinematic

boundary condition is determined by requiring that boundary points remain boundary points. Therefore if $z = \eta(x,t) - d$ is the form of the displaced lower surface,

$$\frac{D}{Dt}\left(z - \eta(x,t)\right) = 0 \tag{6}$$

where $\frac{D}{Dt}$ is the material derivative defined by

$$\frac{D}{Dt} = \frac{\partial}{\partial t} + u\frac{\partial}{\partial x} + w\frac{\partial}{\partial z} \tag{7}$$

Neglecting second order terms in η, ω we have from (6)

$$w = \frac{\partial \eta}{\partial t} = \frac{\partial \omega}{\partial z} \text{ at } z = -d \tag{8}$$

The second boundary condition to be specified at the surface is the dynamic condition. The finite surface elements separate the slab from a constant pressure reservoir. If an individual surface element has a mass, m, then the vertical momentum equation for each of the elements takes the following form

$$m\frac{\partial^2 \eta}{\partial t^2} = \int_0^{\ell} (p_o - p)\, dx - mg \tag{9}$$

Without any loss of generality, we may take the reservoir pressure, $p_o = 0$. This pressure merely establishes a reference level for the entire pressure field.

To determine the pressure field from the velocity field we apply the integrated form of Bernoulli's equation for unsteady irrotational flow

$$\frac{\partial \varphi}{\partial t} + \frac{p}{\rho} + \frac{\nabla\varphi \cdot \nabla\varphi}{2} + gz = 0 \tag{10}$$

This equation is valid everywhere in the slab. In particular, applying it at the fluid side of the finite elements $z = \eta(x,t)-d$ and neglecting second order terms, consistent with a linearized treatment, we obtain

$$\frac{\partial \varphi}{\partial t}(z = -d) + \frac{p}{\rho} + g\eta(x,t) = 0 \tag{11}$$

Therefore,

$$\frac{p}{\rho} = -\left(\frac{\partial \varphi}{\partial t} + g\eta\right) \tag{12}$$

applied at z

In su[illegible]hen, we have the following equations to be solved for the slab $0 \geq z \geq -d$. The differential equation for the velocity potential is Eq. (4)

$$\nabla^2\varphi = 0 \tag{13}$$

with the boundary conditions

$$\frac{\partial \varphi}{\partial z} = 0 \text{ at } z = 0 \tag{14}$$

and

$$\left.\begin{aligned} \frac{\partial \varphi}{\partial z} &= \frac{\partial \eta(x,t)}{\partial t} \qquad (15a) \\ \rho \int_0^{\ell} \left(\frac{\partial \varphi}{\partial t} + g\eta\right) dx &= m\left(g + \frac{\partial^2 \eta}{\partial t^2}\right) \qquad (15b) \end{aligned}\right\} \text{ at } z = d$$

The solution to Eq. (13) which satisfies boundary condition (14) at

$z = 0$ is written as

$$\varphi(x,z,t) = \sum_{n=1}^{\infty} \left\{ A_n(t) \sin(k_n x) + B_n(t) \cos(k_n x) \right\} \cosh(k_n z) \qquad (16)$$

We consider, for the moment, symmetric periodic initial states $z = \eta(x,0)$ of period 2ℓ (twice the finite surface element length) as depicted in Fig. 3. The Fourier representation of this initialization is given as

$$\eta(x,0) = \frac{4\eta_o}{\pi} \sum_{n=1,3,5}^{\infty} \frac{1}{n} \sin\left(\frac{n\pi x}{\ell}\right) \qquad (17)$$

By symmetry, the full time dependent surface perturbation must remain a symmetric square wave given by

$$\eta(x,t) = \frac{4\eta_o(t)}{\pi} \sum_{n=1,3,5}^{\infty} \frac{1}{n} \sin\left(\frac{n\pi x}{\ell}\right) \qquad (18)$$

From Eqs.(15a) (16), and (18) we identify

$$k_n = \frac{n\pi x}{\ell} \ , \ B_n = 0 \qquad (19)$$

and therefore

$$\varphi(x,z,t) = \sum_{n=1,3,5}^{\infty} A_n(t) \sin\left(\frac{n\pi x}{\ell}\right) \cosh\left(\frac{n\pi z}{\ell}\right) \qquad (20)$$

where A_n is determined from Eq. (15a) as

$$A_n(t) = -\frac{4}{\pi}\left(\frac{\partial \eta_o(t)}{\partial t}\right)\left(\frac{1}{n^2}\right)\frac{\ell}{\pi}\frac{1}{\sinh\left(\frac{n\pi d}{\ell}\right)} \tag{21}$$

Equations (20) and (21) therefore represent a solution to Eq. (13) which satisfies the boundary conditions Eqs. (14) and (15a). We must additionally satisfy the dynamic boundary condition, Eq. (15b).

Forming the integrand of Eq. (15b) we have

$$\left(\frac{\partial \varphi}{\partial t} + g\eta\right)_{z=-d} = \frac{4}{\pi}\sum_{n=1,3,5}^{\infty}\left\{-\left(\frac{\ell}{\pi}\right)\frac{\frac{\partial^2 \eta_o(t)}{\partial t^2}}{n^2 \tanh\left(\frac{n\pi d}{\ell}\right)} + \frac{g\eta_o}{n}\right\}\sin\left(\frac{n\pi x}{\ell}\right) \tag{22}$$

We note that if this series vanishes term by term, we recover the classical Rayleigh-Taylor[8] growth rate dispersion relation

$$\omega^2 = \left\{\left(\frac{g\pi}{\ell}\right)n\right\}\tanh\left(\frac{n\pi d}{\ell}\right) \tag{23}$$

for the behavior of $\eta_o(t)$. This implies a growth rate which is dependent upon the particular harmonic wave number $\left(\frac{n\pi}{\ell}\right)$. If each harmonic evolved with a growth rate given by Eq. (23), a square wave initial profile would not remain a square wave.

Applying the full integral form of dynamic condition, Eq. (15b), which balances the vertical force and acceleration for each surface element we obtain

$$- \left(\frac{\ell}{\pi}\right)\left(\frac{\partial^2 \eta_o}{\partial t^2}\right) \sum_{n=1,3,5\ldots} \left\{ \frac{\coth\left(\frac{n\pi d}{\ell}\right)}{n^2} \right\} + g\eta_o \sum_{n=1,3,5\ldots} \frac{1}{n^2}$$

$$= \frac{m\pi^2}{8\rho\ell} \left(g + \frac{\partial^2 \eta_o}{\partial t^2}\right). \tag{24}$$

For $\frac{\pi d}{\ell} >> 1$, we have

$$\frac{\partial^2 \eta_o}{\partial t^2} \left(B + \frac{m\pi^3}{8\rho\ell^2}\right) - \left(\frac{g\pi}{\ell}\right) A\eta_o = - \frac{m\pi^3}{8\rho\ell^2} g \tag{25}$$

where $A = \sum_{n=1,3,5\ldots} \frac{1}{n^2} \sim 1.2288$

and $B = \sum_{n=1,3,5} \frac{1}{n^3} \sim 1.0518$

This provides a growth rate for $\eta_o(t)$ satisfying

$$\omega^2 = \frac{\frac{g\pi}{\ell}\left(\frac{A}{B}\right)}{\left(1 + \frac{m\pi^3}{8\rho\ell^2 B}\right)} \tag{26}$$

The growth rate scales as $\left(\frac{g\pi}{\ell}\right)^{\frac{1}{2}}$ like the Rayleigh-Taylor rate corresponding to the finite element wave length, 2ℓ. The finite element mass, m, is seen to reduce the growth rate inertially as we would anticipate. Assuming the finite elements to be of a material of density ρ^* and thickness d^*,

$$m = \rho^* \, d^* \, \ell \tag{27}$$

or

$$\omega^2 = \frac{\frac{g\pi}{\ell}\left(\frac{A}{B}\right)}{1 + \left(\frac{\pi^3}{8B}\right)\left(\frac{\rho^*}{\rho}\right)\left(\frac{d^*}{\ell}\right)} \tag{28}$$

For an arbitrary surface initialization discretized by finite elements of size ℓ, it is anticipated that the maximum growth rate would scale as $\left(\frac{g\pi}{\ell}\right)^{\frac{1}{2}}$. To demonstrate this, below we consider a few examples.

For an initial symmetric surface perturbation as indicated in Fig. 4 where each wave length (λ) corresponds to three pistons we would anticipate a maximum growth rate ω corresponding to $\lambda/3 = \ell$ which would scale as

$$\omega^2 \sim g\left(\frac{\pi}{(\lambda/3)}\right) = 3g\frac{\pi}{\lambda} \tag{29}$$

When each wave length corresponds to 4 pistons as indicated in Fig. 5, we obtain a maximum growth rate of

$$\omega^2 \sim g\frac{\pi}{(\lambda/2)} \tag{30}$$

as by symmetry it is not possible to populate disturbances of wavelength 2ℓ.

The first non-trivial situation associated with the previous results is for the case where the wavelength of the initial perturbation $\lambda = 6\ell$. This case is illustrated in Fig. 6 where, in addition, it is shown that the surface displacement at any time may be represented as the sum of two symmetric square waves of wave lengths 2ℓ and 6ℓ, respectively.

That is, the surface perturbation is

$$\eta(x,t) = \frac{4}{\pi}\left\{ \eta_1(t) \sum_{1,3,5\ldots}^{\infty} \frac{1}{n} \sin\frac{n\pi x}{\ell} + \eta_3(t) \sum_{1,3,5}^{\infty} \frac{1}{n} \sin\frac{3n\pi x}{\ell} \right\} \tag{31}$$

As before, the velocity potential in the region $0 \le z \le -d$ satisfies

$$\nabla^2\varphi = 0. \tag{32}$$

The boundary conditions are

$$\varphi_z = 0\Big)_{(z=0)}, \tag{33a}$$

$$\eta_t = \varphi_z\Big)_{(z=-d)}, \tag{33b}$$

$$\int_0^{\ell} (\varphi_t + g\varphi_z)dx = 0\Big)_{(z=-d)} \tag{33c}$$

and

$$\int_0^{3\ell} (\varphi_t + g\varphi_z)dx = 0\Big)_{(z=-d)}. \tag{33d}$$

Two dynamic conditions, Eq. (33c) and (33d) are now required to specify the surface pressure balance for the finite elements. We have considered only the case of massless pistons here ($m = 0$). Proceeding as before the solution for the velocity potential which satisfies the differential equation (32) and boundary conditions (33a) and (33b) consistent with the displacement of Eq. (31) is given as

$$\phi(x,z,t) = -\frac{4}{\pi}\left(\frac{3\ell}{\pi}\right)\left\{\eta_1(t)\sum_{n=1,3,5\ldots}\frac{1}{n^2}\frac{\cosh\left(\frac{n\pi z}{3\ell}\right)\sin\left(\frac{n\pi x}{3\ell}\right)}{\sinh\left(\frac{n\pi d}{3\ell}\right)}\right.$$

$$\left. + 3\eta_3(t)\sum_{n=3,9,15\ldots}\frac{1}{n^2}\frac{\cosh\left(\frac{n\pi z}{3\ell}\right)\sin\left(\frac{n\pi x}{3\ell}\right)}{\sinh\left(\frac{n\pi d}{3\ell}\right)}\right\} \tag{34}$$

Applying the dynamic conditions (33c) and (33d), after some algebraic manipulation we obtain

$$\ddot{\eta}_3 = \left(\frac{g\pi}{3\ell}\right)\left(\frac{A}{B}\right)\left(\frac{18}{26}\eta_1 + 3\eta_3\right) \tag{35}$$

and

$$\ddot{\eta}_1 = \left(\frac{g\pi}{3\ell}\right)\frac{A}{B}\left(\frac{24}{26}\right)\eta_1 \tag{36}$$

It is seen that there are now two growth rates ω_1 and ω_3. $\omega_1^2 \sim \frac{g\pi}{3\ell}$ for the fundamental and $\omega_3^2 \sim \frac{g\pi}{\ell} \sim 3\omega_1^2$ for the smaller wavelength square wave. Each above growth rate is seen to scale in a Rayleigh-Taylor sense (Eq. (1)) with its wavelength.

IV. Conclusions

From the preceding analyses, it is seen that the use of a plurality of free-pistons to drive a liquid liner, while eliminating high frequency Rayleigh-Taylor instability at the outer edge of the liner, is still subject to low-frequency positional-instability. The growth of variations in piston positions occurs at rates similar to those that

would be calculated based on the classical Rayleigh-Taylor analysis for wavelengths equal to multiples of twice the piston size; significant quantitative differences, however, do exist. The result of such instability is to provide a nonuniform, asymmetric distribution of fluid momentum, which can have serious consequences for both the quality of the inner surface implosion and the mechanical behavior of the rotating liner implosion system.

V. Acknowledgement

The authors would like to acknowledge many useful discussions with Dr. P. Sprangle.

REFERENCES

1. D. L. Book, et al., "Stabilized Imploding Liner Systems", Sixth IAEA Conference on Plasma Physics and Controlled Nuclear Fusion Research, Berchtesgaden, FRG, 6-13 Oct 1976, Paper E19-1.
2. G. I. Taylor, "The Instability of Liquid Surfaces when Accelerated in a Direction Perpendicular to Their Planes. I", Proc. Roy. Soc. A, 201, 192 (Part I).
3. P. J. Turchi and A. E. Robson, "Conceptual Design of Imploding Liner Fusion Reactors", Proc. of Sixth Symp. on Eng. Problems of Fusion Research, San Diego, Calif., Nov 18-21, 1975, IEEE Publication No. 75CH1097-5-NPS, p. 983.
4. D. L. Book and N. K. Winsor, "Rotational Stabilization of a Metallic Liner", Phys. Fluids, 17, 662 (1974).
5. A. Barcilon, D. L. Book and A. L. Cooper, "Hydrodynamic Stability of a Rotating Liner", Phys. Fluids, 17, 1707 (1974).
6. P. J. Turchi, A. L. Cooper, R. Ford and D. J. Jenkins, "Rotational Stabilization of an Imploding Liquid Cylinder", Phys. Rev. Lett. 36, 1546 (1976).
7. P. J. Turchi, D. J. Jenkins, R. D. Ford and A. L. Cooper, "Rotational Stabilization of the Inner Surface of a Piston-Driven Imploding Liner", NRL Memorandum Report in preparation.
8. John Marshall and Jay Hamil, LASL, private communication.
9. S. Chandreshekar, "Hydrodynamic and Hydromagnetic Stability", Oxford University Press (1961).

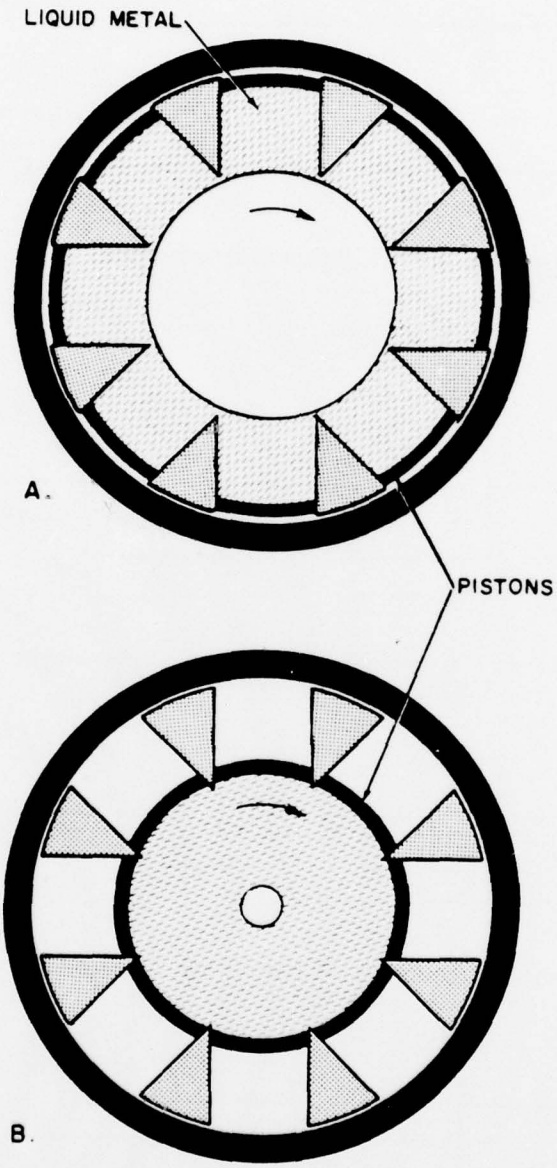

Fig. 1 — Captive liner with radial free pistons

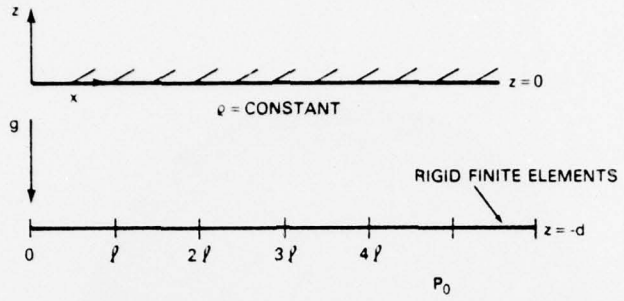

Fig. 2 — Finite element slab model

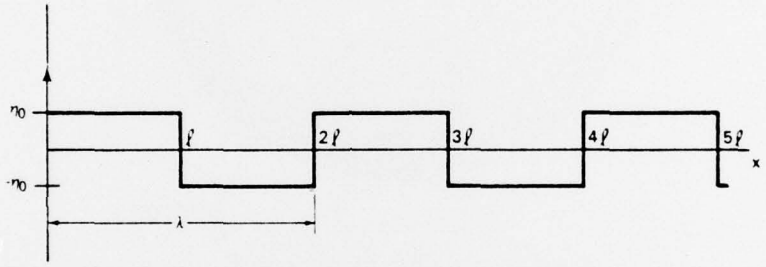

Fig. 3 — Symmetric initial surface displacement for minimum wavelength ($\lambda = 2\ell$)

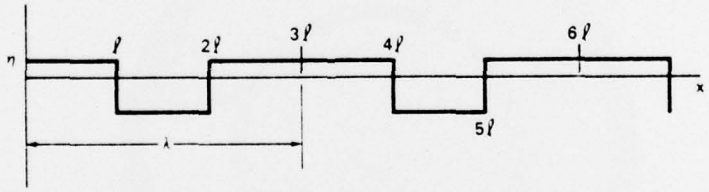

Fig. 4 — Symmetric initial surface displacement for $\lambda = 3\ell$

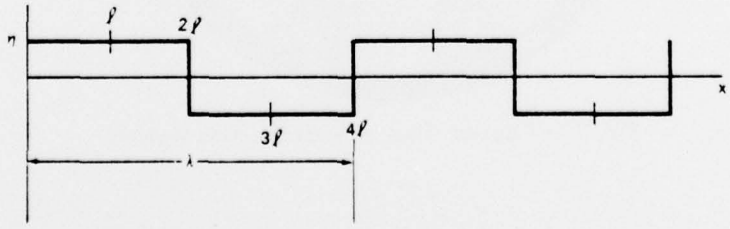

Fig. 5 — Symmetric initial surface displacement for $\lambda = 4\ell$

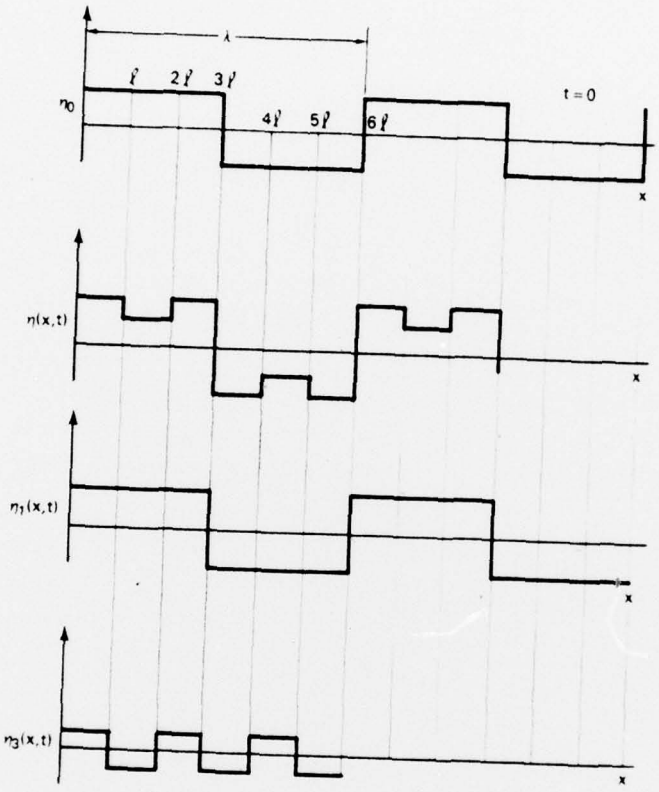

Fig. 6 — Symmetric initial surface displacement and its evolution for $\lambda = 6\ell$